Eur Biophys J (2001) 30: 147–161
DOI 10.1007/s002490000118

ARTICLE

**Jean-Claude Talbot · Eric Thiaudière · Michel Vincent
Jacques Gallay · Odile Siffert · Jean Dufourcq**

Dynamics and orientation of amphipathic peptides in solution and bound to membranes: a steady-state and time-resolved fluorescence study of staphylococcal δ-toxin and its synthetic analogues

Received: 30 July 2000 / Revised version: 25 August 2000 / Accepted: 2 September 2000 / Published online: 20 December 2000

Abstract The environment of both the hydrophilic and hydrophobic sides of α-helical δ-toxin are probed by tryptophanyl (Trp) fluorescence, when self-association occurs in solution and on binding to membranes. The fluorescence parameters of staphylococcal δ-toxin (Trp15 on the polar side of the amphipathic helix) and synthetic analogues with single Trp at position 5 or 16 (on the apolar side) were studied. The time-resolved fluorescence decays of the peptides in solution show that the local environment of their single Trp is always heterogeneous. Although the self-association degree increases with concentration, as shown by fluorescence anisotropy decays, the lifetimes (and their statistical weight) of Trp16 do not change, contrary to what is observed for Trp15. The first step of self-association is then driven by hydrophobic interactions between apolar sides of α-helices, whilst further oligomerization involves their polar side (Trp15) via electrostatic interactions. This is supported by dissociation induced by salt. For all self-associated peptides, the polarity of the Trp microenvironment was not significantly modified upon binding to phospholipid vesicles, as indicated by the small shifts of the fluorescence emission spectra and lifetime values. However, the relative populations of the lifetime classes vary with bound-peptide density similar to the rates of their global motions in bilayers or smaller particles. Quenching experiments by water or lipid-soluble compounds show changes of the orientation of membrane-inserted peptides, from probably dimers lying flat at the interface at low peptide density, to oligomers spanning the membrane and inducing membrane fragmentation at high peptide density.

Keywords δ-Toxin · Fluorescence quenching · Time-resolved fluorescence anisotropy · Mobility · Self-association

Abbreviations *BLM*: black lipid membrane · *DMPC*: 1,2-dimyristoyl-*sn*-glycero-3-phosphocholine · *EDTA*: ethylenediaminetetraacetic acid · *EPC*: egg phosphatidylcholine · *PS*: phosphatidylserine · *MEM*: maximum entropy method · *NATA*: *N*-acetyltryptophanamide · *NO-5PC*: l-palmitoyl-2-(5-doxylstearoyl)-*sn*-glycero-3-phosphocholine · *NO-12PC*: l-palmitoyl-2-(12-doxylstearoyl)-*sn*-glycero-3-phosphocholine · *SUV*: small unilamellar vesicles · *TFA*: trifluoroacetic acid

Introduction

Staphylococcal δ-toxin is a membrane-active peptide of 26 amino acid residues, containing a single tryptophanyl (Trp) residue at position 15. It is lytic towards eukaryotic cells (Kreger et al. 1971; Freer et al. 1984). In aqueous solution, it self-aggregates and folds as a well-defined amphipathic α-helix in the micromolar concentration range, and dissociates into unstructured monomers at very low concentrations (Garone et al. 1988; Thiaudière et al. 1991).

Self-associated δ-toxin interacts strongly with zwitterionic or negatively charged lipids (Morgan et al. 1986; Thiaudière et al. 1991) and is always α-helical whatever its secondary or quaternary structure in solution (Lee et al. 1987; Thiaudière et al. 1991). Although a single mechanism for the expression of its lytic potency has already been proposed (Freer and Birkbeck 1982; Mellor

J.-C. Talbot (✉) · E. Thiaudière[1] · J. Dufourcq
Centre de Recherche Paul Pascal, CNRS,
Av. A. Schweitzer, 33600 Pessac, France
E-mail: talbot@crpp.u-bordeaux.fr

M. Vincent · J. Gallay
LURE, CNRS-CEA-MEN,
Université de Paris Sud, 91405 Orsay, France

O. Siffert
Unité de Chimie Organique, Institut Pasteur,
25 rue du Dr Roux, 75015 Paris, France

Present address:
[1]Unité de Résonance Magnétique des Systèmes Biologiques,
Université de Bordeaux II, 146 rue Léo Saignat,
33076 Bordeaux Cedex, France

et al. 1988), δ-toxin can induce cell lysis in at least three different ways. First, membrane disruption can occur, as described for bee venom melittin which fragments cell membranes (Katsu et al. 1988, 1989) or phosphatidylcholine bilayers (Dufourcq et al. 1986). Secondly, transmembrane channels can be induced: ions and/or small-sized molecules may cross the cell membrane, producing a colloid-osmotic effect (Freer and Birkbeck 1982; Mellor et al. 1988). Finally, a wedge effect as first described by Dawson et al. (1978) for melittin and further documented by Weaver et al. (1992) can also be proposed. The insertion of δ-toxin in the membrane may cause local perturbation of the lipid packing without necessarily forming a channel (Dufourc et al. 1990), which is able to induce a colloid-osmotic lysis of the cell. The lack of correlation between channel and lytic activities shown by different δ-toxin analogues also favours this last mechanism (Kerr et al. 1995).

In an attempt to provide further information about the mechanism of the interaction of δ-toxin with membranes, a series of peptide analogues were synthesized (Alouf et al. 1989), with a simplified composition preserving the amphiphilic character (Fig. 1) of the α-helical conformation that natural δ-toxin can adopt on increasing its concentration or on binding to membranes (Alouf et al. 1989; Thiaudière et al. 1991). All the hydrophobic residues were changed to Leu, well known to favour helix formation (DeGrado et al. 1981), while the polar ones were unchanged. As for the study of the binding of a series of 17-residue-long synthetic peptides to calmodulin (O'Neil et al. 1987), the chosen positions for the only-Trp substitution allow us to probe either the hydrophilic (position 15) or lipophilic (positions 5 and 16) surfaces of this amphipathic helix (Fig. 1).

The changes in the environment of the Trp, induced by the binding of the peptide to membranes, were monitored by measurement of the excited state lifetime distributions and the rotational correlation time distributions of the free and membrane-bound peptides by means of the time-resolved fluorescence technique. It is shown that, despite the very small changes in the average polarity of the microenvironment of Trp upon binding to membranes detected by static fluorescence, large modifications of the excited state population distributions of Trp, whatever its position, are observed. These changes are dependent on the hydrophilic/lipophilic position of Trp on the amphipathic helix. The excited state lifetime distributions of Trp15-peptide in the bound state differ from those of Trp16- or Trp5-peptides which display similar behaviour. The longest rotational correlation time changes significantly upon binding to lipids according to the initial self-association state in solution and to the lipid-to-peptide molar ratio. Quenching experiments by CsCl and doxyl groups anchored on C5 or C12 of the *sn*-2-acyl chain of phosphatidylcholine indicate also that inserted peptides can reorient. Light scattering experiments show that δ-toxin induces changes in the size of mixed phosphatidylcholine/phosphatidylserine vesicles. All these changes, which depend on the surface density of peptides in bilayers, can be correlated with the orientation of the inserted peptides.

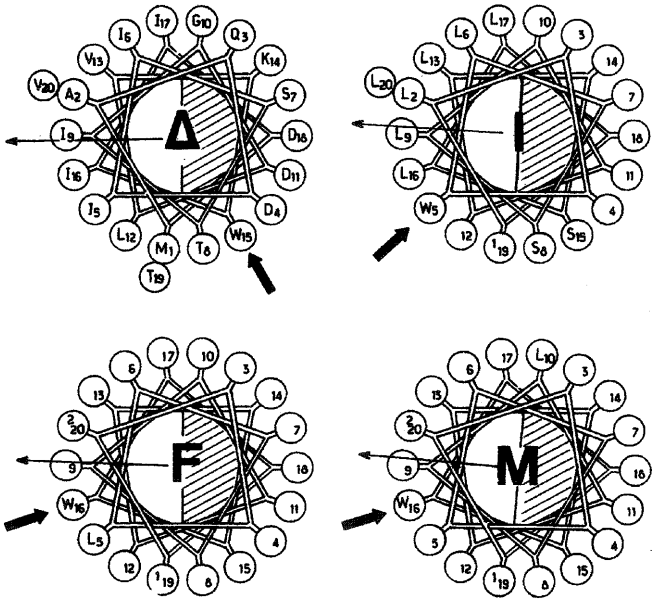

Fig. 1 Schiffer-Edmundson projections of segment 1–20 of synthetic δ-toxin Trp15 ("Δ") and analogues with Trp in position 5 ("I") and 16 ("F" and "M") in α-helical conformation, which exhibit an ideal segregation of polar (*hatched sector*) and apolar residues. Only further substitutions in one sequence compared to the previous one in the series Δ, I, F, M are specified. The *thin arrows* represent the hydrophobic moments calculated from the "consensus scale" of hydrophobicity of the amino acid residues according to Eisenberg et al. (1982). Trps are indicated by *thick arrows*

Materials and methods

δ-Toxin and synthetic analogues

δ-Toxin and analogues I and F (Table 1) were synthesized, purified and characterized earlier (Alouf et al. 1989). In peptide I, all apolar side-chains from 2 to 20 are replaced by Leu, and Trp is shifted from position 15 in δ-toxin to position 5. Peptide F has the same sequence as peptide I but Trp5 and Leu16 are exchanged. Peptide M was synthesized for this study, purified by HPLC and characterized by amino acid analysis as previously (Alouf et al. 1989) and by fast atom bombardment mass spectrometry; the expected molecular mass (3062 Da) was measured. The only difference in sequence of peptide M compared with peptide F is the replacement of Gly10 by a Leu. Like δ-toxin, peptide F is formylated whereas peptides I and M are not. The lytic activity and voltage-induced pore formation are similar for δ-toxin, peptides F and M, but pore stability is less when the N-terminal Met is unformylated (Kerr et al. 1995). These peptides are likely to be in an α-helix from residue 7 to 23 when self-associated (Dufourcq et al. 1999) and δ-toxin has been shown to be in an α-helix from residue 5 to 23 when bound to lipid micelles (Lee et al. 1987). Their Schiffer-Edmundson projections and the orientation of their hydrophobic moments (Eisenberg et al. 1982) are shown in Fig. 1.

Table 1 Sequences of δ-toxin and peptides I, F and M. Only the differences from the preceding sequence are reported

	1				5					10					15	16				20						26
δ-Toxin	fM	A	Q	D	I	I	S	T	I	G	D	L	V	K	[w]	I	I	D	T	V	N	K	F	T	K	K
I	M	L	–	–	[w]	L	–	S	L	–	–	–	L	–	S	L	L	–	–	L	–	–	–	–	–	–
F	fM	–	–	–	L	–	–	–	–	–	–	–	–	–	–	[w]	–	–	–	–	–	–	–	–	–	–
M	M	–	–	–	–	–	–	–	–	L	–	–	–	–	–	[w]	–	–	–	–	–	–	–	–	–	–

Chemicals

Natural phospholipids were purified in the laboratory (egg phosphatidylcholine, EPC) according to Singleton et al. (1965) or purchased (phosphatidylserine, PS) from Lipid Products (Nutfield, UK). Co-lyophilized lipids were suspended in 20 mM Tris-HCl buffer (pH 7.5)+1 mM ethylenediaminetetraacetic acid (EDTA) and sonicated at room temperature until the best clearing was obtained. l-Palmitoyl-2-(5-doxylstearoyl)-*sn*-glycero-3-phosphocholine (NO-5PC) was a generous gift of Dr. Zackowski (Institut de Biologie Physicochimique, Paris, France) and l-palmitoyl-2-(12-doxylstearoyl)-*sn*-glycero-3-phosphocholine (NO-12PC) was from Avanti Polar Lipids (Alabaster, Ala., USA). *N*-Acetyltryptophanamide (NATA) was from Sigma (St. Louis, Mo., USA) and CsCl from Alfa Products (Danvers, Mass., USA).

Fluorescence emission spectra

Corrected fluorescence emission spectra were recorded on a SLM 8000 spectrofluorometer (Urbana, Ill., USA) with an excitation wavelength of 280 nm (bandwidth: 8 nm). Buffer blanks were always subtracted under the same experimental conditions in order to eliminate Rayleigh and Raman scattering.

Light scattering experiments

Aliquots of peptide M [1.8 mM in 0.1% trifluoroacetic acid (TFA)] were added to small unilamellar vesicles (SUV) of PC:PS (4:1) obtained by sonication in Tris buffer (pH 7.2). Scattered light intensities were recorded at 90° in the spectrofluorometer (280 nm excitation and emission wavelengths, 4 nm bandwidth) concomitantly with the emission fluorescence spectra of the peptide. Data were acquired after stabilization of the signal, i.e. after 0.5–8 h, under magnetic stirring.

Time-resolved fluorescence spectroscopy

Tryptophan was illuminated by pulsed excitation provided by the positon storage ring Super-Aco (Anneau de Collision d'Orsay) working in a two-bunch mode. The frequency of the excitation pulse was 8.33 MHz and a typical value of 0.6 ns was monitored for the full width at half-maximum of the instrumental response. The excitation wavelength was selected at 295 nm by a grating monochromator and vertically polarized through a Glan-Thompson prism. The decays of the parallel $I_{vv}(t)$ and of the perpendicular $I_{vh}(t)$ intensities were collected alternatively on the instrument set-up as previously described (Kuipers et al. 1991) by the single-photon counting method (Yguerabide 1972; Wahl 1975). Full time scales of about 30 ns were routinely used for decay accumulation.

The total fluorescence intensity decays $T(t)$ were reconstructed from the decays $I_{vv}(t)$ and $I_{vh}(t)$ as previously (Li de la Sierra et al. 1992). Then they were analyzed using the maximum entropy method (MEM) (Livesey and Brochon 1987; Livesey et al. 1987; Vincent et al. 1988; Merola et al. 1989; Gentin et al. 1990; Kuipers et al. 1991) with an initial set of 150 lifetime values, equally spaced in a logarithmic scale.

The fluorescence anisotropy decay parameters were calculated also by MEM. It was assumed that every type of excited state is responsible in the same way for every type of depolarization process and possesses the same fundamental anisotropy value A_0 (Vincent and Gallay 1991; Li de la Sierra et al. 1992). Anisotropy decays $A(t)$ can be expressed in terms of order parameters S_i according to the equation of Ichiye and Karplus (1983), which describes these decays with two discrete rotational correlation times θ_1 and θ_2 for two anisotropic local motions and a longer correlation time θ_3 for the isotropic movement of the whole molecule. Their equation can be generalized for n any movements as:

$$A(t) = A_0 \prod_{i=1}^{n} \left[(1 - S_i^2) e^{-t/\theta_i} + S_i^2 \right] = \sum_{i=1}^{n} \beta_i e^{-t/\theta_i} \quad (1)$$

if $\theta_i \ll \theta_{i+1}$. S_i is the order parameter related to the movement of rotational correlation time θ_i, and ${S_n}^2 = 0$ if θ_n is not infinite, $1 \geq {S_i}^2 \geq 0$, from a fixed orientation (maximum anisotropy) to unordered (isotropic) movements in a (hemi)sphere for the "wobbling in a cone" model defined by Lipari and Szabo (1982), Kinosita et al. (1977) and Kawato et al. (1977).

The right-hand side of Eq. (1) is identical with the anisotropy decay reconstructed from the distribution profile obtained by MEM on rewriting it as a sum of exponential functions, where θ_i is the barycentre value of each peak of the distribution profile and β_i is the initial anisotropy relative to each peak:

$$\beta_i = \int_{\theta_{i\,\min}}^{\theta_{i\,\max}} \beta(\theta)\, d\theta \quad (2)$$

From Eq. (1) it appears that the order parameter related to each movement "i" is:

$$S_i = \left(\frac{\sum_{j=i+1}^{n} \beta_j}{\sum_{j=i}^{n} \beta_j} \right)^{1/2} \quad (3)$$

which depends on the semi-angle γ_i of the cone surrounding motions in the "wobbling in a cone" model by:

$$S_i = (1/2) \cos \gamma_i (1 + \cos \gamma_i) \quad (4)$$

It must be noticed that this model applies to only one molecular species whose fluorophore undergoes all the motions characterized by all the θ_is. If different species were observed, the only pertinent parameters are the correlation times θ_i and their statistical weights β_i.

Equation (4) can give access to γ_{max} from:

$$S_{global} = \left(\frac{A_\infty}{A_0} \right)^{1/2} = \left(\frac{\beta_n}{\sum_{i=1}^{n} \beta_i} \right)^{1/2} = (1/2) \cos \gamma_{max} (1 + \cos \gamma_{max}) \quad (5)$$

when it retains some anisotropy for $t \to \infty$, i.e. when the nth movement is anisotropic in the fluorescence time scale.

If the fastest movement escaped to measurement owing to scattered light or a lack of temporal resolution, the experimental decay is:

$$A(t) = \sum_{i=2}^{n} \beta_i e^{-t/\theta_i} \quad (6)$$

and $\sum_{i=2}^{n} \beta_i = A_{0\,\text{apparent}} < A_0$. The order parameter of that movement is:

$$S_1 = \left(\frac{A_{0\,\text{apparent}}}{A_0}\right)^{1/2} \quad (7)$$

and A_0 can be measured by steady-state fluorescence anisotropy in the absence of movement, i.e. at high viscosity η and low temperature T, through extrapolation of a Perrin plot to $T/\eta \to 0$.

Fluorescence quenching experiments

CsCl was added to peptides from a 5.6 M stock solution in 20 mM Tris-HCl buffer (pH 7.5)+1 mM EDTA. The collisional quenching efficiency of tryptophan fluorescence by Cs^+ is defined as $(I_0/I) - 1$, where I_0 and I represent the fluorescence in the absence and in the presence of quencher, respectively. The efficiency is related to quencher concentration by the Stern-Volmer equation $(I_0/I) - 1 = K[Q]$, with K, the Stern-Volmer constant, equal to $k_q\tau_0$ (k_q is the second-order kinetic constant of the quenching induced by bimolecular collision; τ_0 is the lifetime of Trp in the absence of quencher Q). When these graphs are not linear, they are fitted by:

$$\frac{I_0}{I} - 1 = \frac{K[Q]f_a}{1 + K[Q](1 - f_a)} \quad (8)$$

where f_a is the only Trp fraction accessible to Cs^+.

The tryptophan fluorescence of bound peptides was quenched in vesicles made of co-lyophilized doxylated phosphatidylcholines and EPC. Saturation curves obtained by measuring the change of the tryptophan fluorescence as a function of the concentration of pure egg phosphatidylcholine vesicles are compared to those monitored in the presence of mixed phosphatidylcholine doxylated-phosphatidylcholine vesicles. The model which accounts for the binding of these peptides observed via fluorescence measurements was described previously (Thiaudière et al. 1991). Two spectroscopically distinct bound states are present, one (molar fraction α) with the same quantum yield Φ_F and degree of self-association n as free peptides, the other one, "inserted" (molar fraction α'), with an enhanced quantum yield $\left(\Phi_B^0\right)'$ and half of the self-association degree n'. This part, sensitive to lipid binding, is assumed to be the only one that may be quenched. It is calculated from the following characteristics of the bindings: partition coefficients "γ" $= 5 \times 10^5$, 5×10^5, 7×10^4, equilibrium constant K between the two bound states 10, 6, 21 for δ-toxin, peptide F and peptide I, respectively (Thiaudière 1990; Thiaudière et al. 1991); n is estimated from time-resolved fluorescence anisotropy measurements. The quenching efficiency E is then calculated as:

$$E = 1 - \frac{\left(\Phi_B^Q\right)'}{\left(\Phi_B^0\right)'} \quad (9)$$

where $\left(\Phi_B^Q\right)'$ is the quantum yield of the fraction α' in the presence of quencher at the same lipid to inserted peptide molar ratio R_b'. It should be constant and is related to measured intensities $I_{R_i}^0$ and $I_{R_i}^Q$ in the absence and in the presence of quencher, respectively, by:

$$E = \frac{I_{R_i}^0 - I_{R_i}^Q}{I_{R_i}^0 - I_0^0(1 - \alpha')} \quad (10)$$

where $I_0{}^0$ is the intensity in the absence of lipid and R_i is the total lipid to peptide molar ratio inducing inserted fraction α'.

Results and discussion

Light scattering changes related to peptide M in solution and to lipids in the presence of this peptide

When peptide M (Trp16), in a clear stock solution at pH 2.1, is diluted to 7.2 μM into Tris buffer (pH 7.2), a large increase in light scattering develops over 40 min. This is consistent with the occurrence of very large aggregates. Then, the increase of NaCl concentration step by step up to 1.9 M induces successive slow decreases (over several hours) of scattered light, indicative of partial dissociation of the peptide into new oligomers. This proves the part of ionic interactions between peptidic chains, in agreement with what was assumed earlier (Thiaudière et al. 1991).

When peptide M (from the same stock solution) is added to PC:PS (4:l) SUV, no increase of the scattering is observed until the total lipid to peptide molar ratio $R_i = 20$. Then, a drastic decrease occurs with further additions of peptide M between $R_i = 14$ and $R_i = 7$ (Fig. 2), which proves the fragmentation of SUV into smaller particles very similar to the vesicle to disc-shape transition documented for melittin (Dufourcq et al. 1986) and very recently for δ-toxin-DMPC (1,2-dimyristoyl-*sn*-glycero-3-phosphocholine) complexes (Lohner et al. 1999). At $R_i = 5$, the increase of the

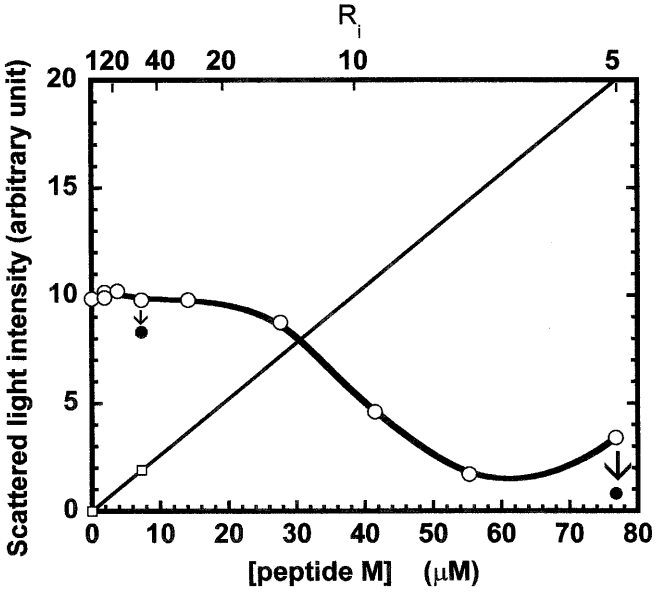

Fig. 2 Changes of the light scattered by lipid vesicles upon addition of various amounts of a stock solution of Trp16-peptide M in 0.1% TFA. $\lambda_{ex} = 280$ nm; [PC-PS] = 400 μM; PC-PS sonicated vesicles (4:1 mol:mol) in 20 mM Tris-HCl buffer (pH 7.2)+1 mM EDTA at 20 °C. The *straight full line* shows the expected change in scattered light calculated for free peptide M from what was observed at 7.2 μM (□). As the degree of self-association of these peptides is increasing with concentration (Thiaudière et al. 1991), these calculated scattered intensities are minimized where [peptide M] > 7.2 μM. *Arrows*: effect of NaCl addition up to 1.9 M

scattered light intensity is accounted for by the occurrence of 10% unbound peptide, as suggested by the effect of bringing the NaCl concentration from 0 to 1.9 M. The scattered light intensity is then decreased by about 77%, a greater value than what is expected from the observed decrease (18%) on pure EPC vesicles (not shown) or at other values of R_i, because of the change in refractive index.

Fluorescence lifetimes of the single Trp of the peptides in solution

The decays of the single-Trp emission, for each peptide, whatever its position in the amino acid sequence and whatever the concentration in Tris buffer, are multi-exponential (Fig. 3 and Tables 2 and 3). Three resolved lifetime classes are shown by MEM analysis. These discrete lifetime classes suggest the existence of slowly exchangeable conformers. Above 2 μM, their barycentres, τ_i, and their relative contributions, α_i, do not vary significantly whatever the Trp position on the hydrophobic side of the amphipathic helices (Thiaudière et al. 1991) in this range of concentration. Unfortunately, measurements under 1 μM gave data without good confidence. In the case of the "hydrophilic" Trp15 δ-toxin (Fig. 4), significant changes occur until 5 μM, mainly in the relative distribution of the two smallest lifetimes, while the highest one decreases from 7 to around 4 ns. These observations indicate the existence of quenching interactions likely due to the presence of a Lys (Chen and Barkley 1998), which may be Lys14 of another α-helical chain in the vicinity of Trp15. Final values are reached at higher concentrations than for the Trp16 analogue, in agreement with our previous description of δ-toxin self-association (Thiaudière et al. 1991). Hydrophobic interactions first induced tetramers, which can further self-associate via their polar sides and

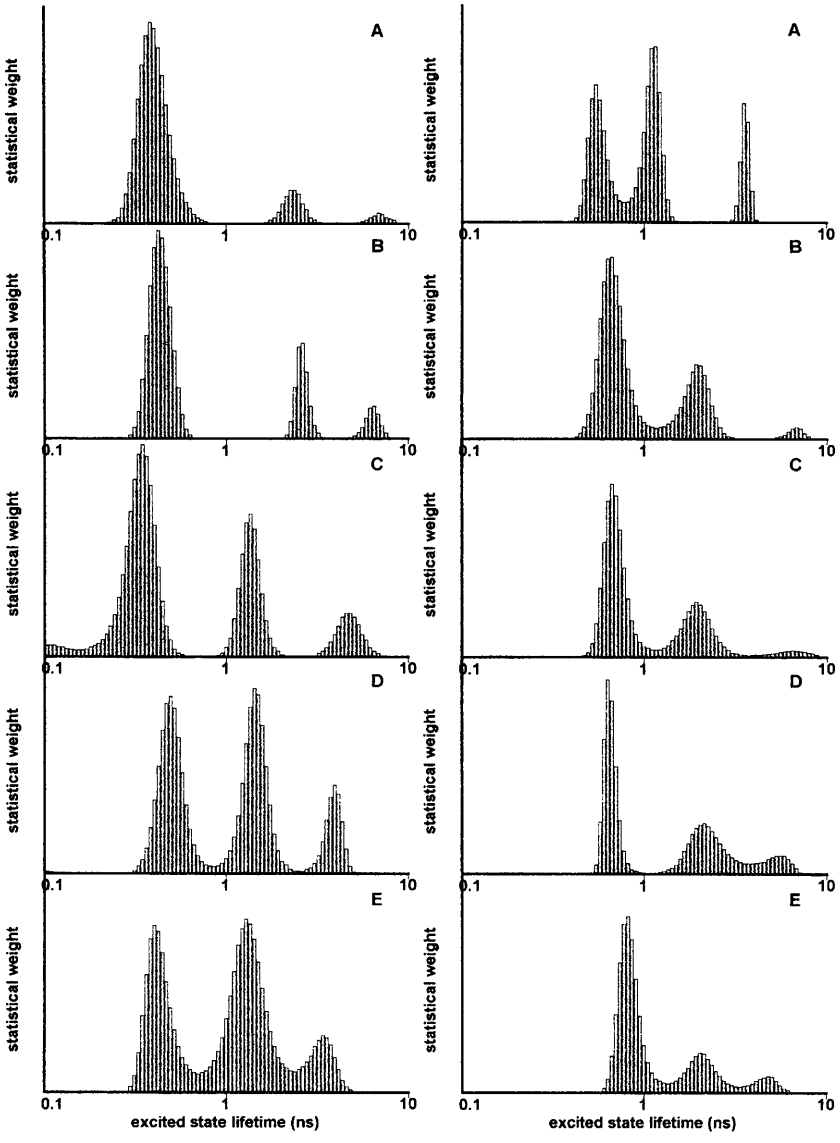

Fig. 3A–E Distribution profiles of Trp lifetimes calculated by MEM analysis of total fluorescence intensity decays of peptides in solution. Trp15-δ-toxin (*left*), Trp16-peptide M (*right*). **A** 0.5 μM, **B** 1 μM, **C** 2 μM, **D** 5 μM, **E** 20 μM. Data are listed in Table 2. Experimental conditions: see Table 3

Table 2 Changes of fluorescence decay parameters of δ-toxin and analogue M as a function of their concentration. α_i and τ_i are the statistical weights and barycentres of the distribution profiles of fluorescence lifetimes shown in Fig. 3

Peptide	Trp	[Peptide] (μM)	α_1	α_2	α_3	τ_1 (ns)	τ_2 (ns)	τ_3 (ns)
δ-Toxin	15	0.5	0.86	0.11	0.03	0.41	2.4	7.2
M	16		0.38	0.46	0.16	0.56	1.1	3.6
δ-Toxin	15	1	0.73	0.19	0.08	0.43	2.6	6.4
M	16		0.68	0.29	0.03	0.65	1.9	6.8
δ-Toxin	15	2	0.60	0.28	0.12	0.33	1.3	4.8
M	16		0.65	0.31	0.04	0.69	2.0	6.4
δ-Toxin	15	5	0.43	0.42	0.15	0.49	1.4	3.8
M	16		0.52	0.37	0.11	0.65	2.3	5.3
δ-Toxin	15	20	0.36	0.51	0.13	0.43	1.3	3.3
M	16		0.69	0.23	0.08	0.82	2.1	4.6

Table 3 Total fluorescence intensity decay parameters of δ-toxin and analogues F, M and I in aqueous solution in 20 mM Tris-HCl buffer (pH 7.5) + 1 mM EDTA or in interaction with mixed PC-PS vesicles (4:1 mol:mol) to make negligible the contribution of free peptides. Excitation wavelength: 295 nm (bandwidth 5 nm); emission wavelength: 350 nm (bandwidth 10 nm); temperature 20 °C. Data analysis was performed with MEM with a sum of exponential functions. $\bar{\tau} = \sum_i \alpha_i \tau_i$ is the mean lifetime, α_i is the statistical weight of each distribution of τ around τ_i

Peptide	Trp	R_i	α_1	α_2	α_3	τ_1 (ns)	τ_2 (ns)	τ_3 (ns)	$\bar{\tau}$ (ns)	χ^2	λ_{max} (nm)
δ-Toxin (20 μM)	15	0	0.36	0.51	0.13	0.43 ± 0.08	1.3 ± 0.3	3.3 ± 0.6	1.3 ± 0.3	1.04	340 ± 1
		20	0.29	0.39	0.32	0.22 ± 0.08	0.9 ± 0.2	3 ± 1.3	1.4 ± 0.5	1.16	342 ± 1
F (20 μM)	16	0	0.50	0.35	0.15	0.40 ± 0.08	1.5 ± 0.3	4.2 ± 0.5	1.3 ± 0.2	0.99	334 ± 1
		20	0.16	0.34	0.50	0.22 ± 0.01	1.4 ± 0.1	4.0 ± 0.3	2.5 ± 0.1	1.04	332 ± 1
M (20 μM)	16	0	0.69	0.23	0.08	0.8 ± 0.1	2.1 ± 0.4	4.6 ± 0.7	1.4 ± 0.3	1.04	329 ± 1
		20	0.18	0.37	0.45	0.78 ± 0.03	2.6 ± 0.3	4.5 ± 0.4	3.2 ± 0.3	1.55	332 ± 1
I (20 μM)	5	0	0.49	0.34	0.17	0.37 ± 0.03	1.3 ± 0.2	3.3 ± 0.6	1.2 ± 0.2	1.12	337 ± 1
		20	0.33	0.33	0.34	0.6 ± 0.1	1.9 ± 0.4	4.3 ± 0.8	2.3 ± 0.4	1.08	334 ± 1

electrostatic interactions, finally enabling the partial shielding of Trp15 ($\lambda_{em} = 340$ nm). This can explain also why its lifetime values are totally different from those measured for NATA and Trp in water (Ross et al. 1981). At high concentration, the lifetimes and their relative distributions observed herein are similar to those obtained previously by Garone et al. (1988); the major component is the mean lifetime for the "hydrophilic" Trp15 of δ-toxin and the shortest one for "hydrophobic" Trp5 and Trp16.

Anisotropy decays of the single Trp of the peptides in solution

The time-resolved fluorescence anisotropy decay measurements provide some interesting data to document the aggregation of these peptides in solution (Table 4). Unstructured monomers should display rotational correlation times from l ns (without hydration) up to about 1.5 ns as, for instance, ACTH (1–24), monomeric glucagon (Gallay et al. 1987) or melittin (John and Jähnig 1988), which are of similar size.

The analysis of the anisotropy decays of synthetic δ-toxin and peptide M at 20 μM shows the existence of two or three measurable components, respectively, and a very long or infinite one (Table 4). This component proves the presence of large aggregates, in agreement with what was already observed for natural δ-toxin by sedimentation equilibrium analysis (Thiaudière et al. 1991). The component between 1 and 5 ns could represent either the whole movement of smaller particles or nanosecond flexibility in the aggregates. In this last case, two restricted (~30°) fast movements in the subnanosecond time scale (one measurable of 0.1–0.5 ns and a shorter one evidenced by the lack in total anisotropy) could be attributed to the local motions of the indole ring. On dilution of peptide M (Fig. 5) under 2 μM, the infinite component disappears on behalf of a ca. 2.6 ns component at 1 μM and 1.15 ns at 0.5 μM, which reflects the dissociation of the very large aggregates into dimers and finally into monomers. On dilution, δ-toxin exhibits similar behaviour (Fig. 5). Measured rotational correlation times are in good agreement with the mean molecular masses expected from the isodesmic self-association model already proposed (Fig. 4 in Thiaudière et al. 1991), but they are less polydisperse than expected and dimers seem to occur.

Peptide F, which differs from M only by a Gly10 → Leu substitution and the lack of a formyl group on the N-terminus, shows correlation times similar to those observed for δ-toxin, except that the infinite rotational correlation time changes into a value of 8.2 ns, indicative of smaller oligomers.

Finally, for peptide I, the longest correlation time value is only 5.4 ns, characteristic of the smallest maxi-

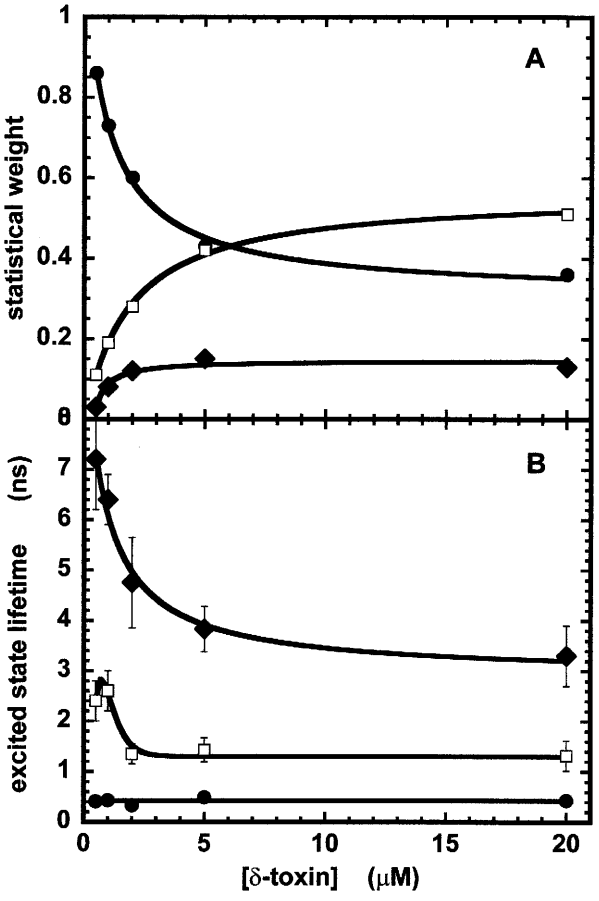

Fig. 4 Effects of concentration on the fluorescence decay parameters of δ-toxin listed in Table 2: (●) shortest, (□) middle and (◆) longest decays. Experimental conditions: see Table 3

mum association degree (4–5) occurring in this series of 26-residue-long peptides. In this peptide I, all the other components are too short to represent the motion of smaller aggregates or even monomers; they are due to fast reorientation internal motions within the oligomeric form of the peptide.

Fluorescence lifetimes of the single Trp of the peptides: effect of binding to phospholipid vesicles

For all these peptides, drastic effects on the fluorescence intensity decays are observed upon binding to membrane vesicles, by contrast to the modest changes of the fluorescence emission spectra (Alouf et al. 1989). Analyses of the fluorescence decays show weak changes in the excited state lifetimes but very large differences in their proportions (Table 3). At 20 μM peptide and at a lipid to peptide molar ratio $R_i = 20$, the binding to lipid vesicles decreases to a large extent the contribution of the shortest-lived species to the benefit of the longest-lived, less quenched, excited state population (Table 3). This effect, which is observed for all the peptides, is smaller for the less buried Trp5 of the oligomer of peptide I and for δ-toxin in which the Trp15 is located on the hydrophilic side of the amphipathic helix. Nevertheless, these data suggest that the peptide-peptide interfaces (either hydrophobic or hydrophilic) in the hydro-soluble aggregates are disturbed upon binding to the membrane. These differences induce significant increases of the mean lifetimes (Table 3) of Trps on the apolar side of the helix (Trp5 of peptide I and Trp16 of peptides F and M). On the contrary, the mean lifetime of the "polar" Trp15 of δ-toxin is poorly enhanced. These

Table 4 Fluorescence anisotropy decay parameters of δ-toxin and analogues F, M and I under the same experimental conditions as in Table 2 See Materials and methods for the meaning of the different parameters

Peptide	Trp	R_i	β_2	β_3	β_{max}	A_0 app[a]	γ_1 (°)	γ_2 (°)	γ_3 (°)	γ_{max} (°)	θ_2 (ns)[b]	θ_3 (ns)[b]	θ_{max} (ns)[b]	χ^2
δ-Toxin (20 μM)	15	0	0.063	–	0.095	0.158	26	33	–	90 or 180	0.47 ± 0.08	–	20 ± 3	1.03
		20	0.007	0.047	0.074	0.128	33	11	32	46	0.40 ± 0.02	2.65 ± 0.06	∞	1.12
F (20 μM)	16	0	–	0.028	0.052	0.080	45	–	30	90 or 180	–	0.95 ± 0.03	8.2 ± 0.4	0.98
		20	0.050	0.095		0.145	29	30	90 or 180		1.11 + 0.07	32 ± 5		1.07
M (20 μM)	16	0	0.037	0.026	0.069 and 0.005	0.137	31	26	25	68 and 76	0.45 ± 0.06	1.0 ± 0.2	5.4 ± 1.0 and ∞	0.98
		20	0.010	0.023	0.103	0.136	31	13	21	39	0.60 ± 0.02	2.10 ± 0.09	∞	1.36
I (20 μM)	5	0	0.044	0.031	0.072	0.147	29	27	28	90 or 180	0.17 ± 0.03	0.72 ± 0.06	5.4 ± 0.1	1.14
		20	–	0.028	0.090	0.118	36	–	24	42	–	3.35 ± 0.03	∞	1.14

[a] The actual initial anisotropy A_0 in 91% glycerol at −38 °C is 0.218 (Vincent et al. 1988). Total measured anisotropies, $A_{0\ app}$, are smaller than A_0. So, the fastest correlation time θ_1 (if unique) is not measured but its angular amplitude γ_1 may be calculated (see Materials and methods)

[b] A spherical monomer of $M = 3000$ without hydration would exhibit $\theta_{max} = 0.96$ ns in water at 20 °C and about 30–50 ns in fluid lipids. Then, short correlation times likely related to indole motion are pooled under θ_2 (with $\beta_2\gamma_2$); intermediate ones (around 1 ns in solution and up to 50 ns in lipids), likely related to the motion of monomers or of the peptide backbone in oligomers, are pooled under θ_3 (with $\beta_3\gamma_3$); θ_{max} (with $\beta_{max}\gamma_{max}$) reflect the global motion of (self-associated) peptides

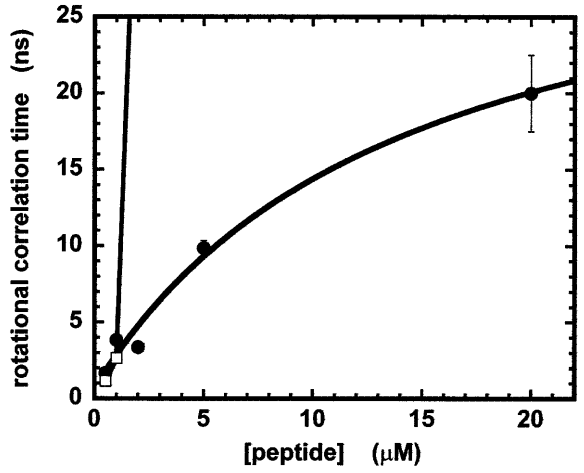

Fig. 5 Effects of concentration on the longest correlation times giving account of the global motion of peptides in solution: (●) δ-toxin, (□) peptide M. Experimental conditions: see Table 3

changes agree with those we observed in the static fluorescence intensity upon binding (Alouf et al. 1989).

Upon binding of aggregated peptide M to lipid vesicles, both the highest lifetimes are reduced by ~1 ns while the highest one in δ-toxin oligomers is enhanced by 2 ns. This is consistent with very weak environmental changes for the Trp16 from the hydrophobic core of aggregated peptide M to lipid bilayers and more drastic changes for the Trp15 from a less apolar environment in oligomers to the lipid medium. However, the longest excited-state lifetime value for Trp16 is constant (4.15 ± 0.06 ns) and never reaches those observed for Trp in the core of lipid bilayers for transmembrane hydrophobic peptides (6–9 ns; Vogel et al. 1988). The shortest lifetime always remains unchanged, as others after binding. The effect of R_i has been more systematically tested at 5 μM peptide M and δ-toxin. Under these conditions, with PC:PS mixed bilayers, there is no significant free peptide (Thiaudière 1990), so that the observed changes do not reflect binding. They prove changes in the organization of peptides in the inserted state are related to peptide surface density. The main changes are concerned with the statistical weight of the different lifetime classes (Fig. 6). When the density of peptide M in the bilayer decreases, the shortest lifetime disappears (at $R_i = 40$) to the benefit of the longest one. For δ-toxin, both the populations with shortest lifetimes seem to exchange between $R_i = 5$ and $R_i = 20$; no further change occurs. The statistical weight of the longest lifetime never changes on dilution in bilayers.

Anisotropy decays of the single Trp of the peptides: effect of binding to phospholipid vesicles

Fluorescence anisotropy decays of Trp16 provide further support to the hypothesis of dissociation upon binding of oligomeric peptides F (20 μM) (Table 4) and

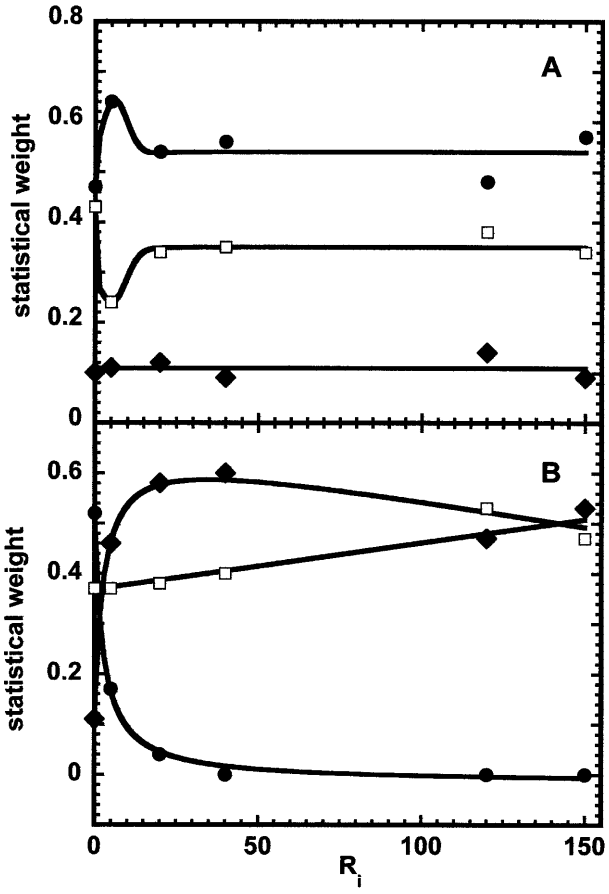

Fig. 6 Effect of the lipid to peptide molar ratio R_i on the statistical weight of the three lifetime classes observed for δ-toxin (**A**) and peptide M (**B**). Peptide concentration: 5 μM; (●) shortest, (□) middle and (◆) longest decays. Experimental conditions: see Table 3

M (2 μM) (data not shown) at $R_i = 20$. A measurable long correlation time (32 ns), without any indication of the presence of an infinite component, is observed. This suggests that reorientation motions of the peptides involve monomers in the membrane and that they are sufficient to totally depolarize the fluorescence emission so that the infinitely slow motion of SUVs still present at this R_i (see Fig. 2) cannot be detected. Taking into account the large polar side of the helix, such monomers are not likely to span the membrane: an orientation parallel to the surface is highly probable. Under the same conditions (Table 4), free tetrameric peptide I (Trp5) and highly self-associated peptide M (Trp16) and δ-toxin (Trp15) do not reach a monomeric bound state since infinite correlation times are observed. Notice that a bound dimeric peptide must show an infinite rotational correlation time compared with the short lifetimes of Trp. In these cases, the movement assigned to the flexibility of the whole peptide chain is slowed down, whereas those of the indole ring are unchanged or too fast to be measured. The amplitudes of local movements are not modified.

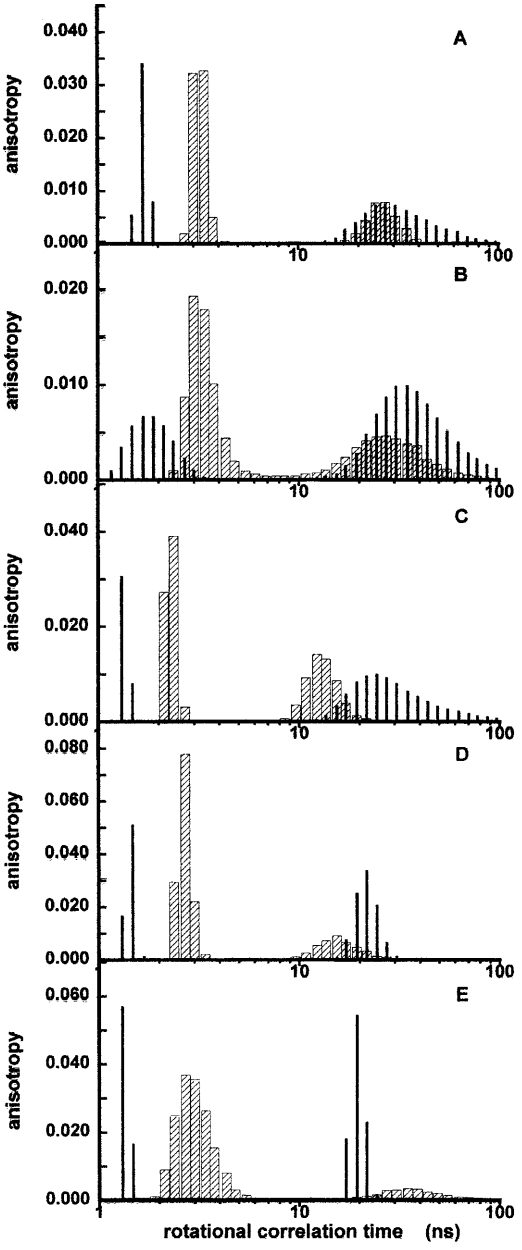

Fig. 7A–E Distribution profiles of Trp rotational correlation times calculated by MEM analysis of polarized fluorescence intensity decays of bound peptides. 5 μM δ-toxin (*hatched bars*) and 5 μM peptide M (*dark bars*). **A** $R_i = 5$, **B** $R_i = 20$, **C** $R_i = 40$, **D** $R_i = 120$, **E** $R_i = 150$. Data are listed in Table 5. Experimental conditions: see Table 3

As shown by Fig. 7 and listed in Table 5, the rotational correlation times of 5 μM bound δ-toxin (Trp15) and peptide M (Trp16) vary with their surface densities. The barycentres of the distributions of the shortest correlation times are significantly longer than in free peptides and reach a minimum plateau value at $R_i \geq 40$. These times are likely attributable to local movements of the Trp in the bilayer. Trps are more immobilized at high peptide density and, surprisingly, this effect is more pronounced for the "hydrophilic" Trp15 (δ-toxin) than for the "hydrophobic" Trp16 (peptide M). This Trp could be exposed to the acyl chains of fluid lipids, in agreement with their maximum emission centred at 332 nm; Trp15 with its maximum emission at 342 nm could be in the less apolar and more constrained environment of the interface between adjacent peptide helices. Another family of much longer correlation times is observed, centred around 14–34 ns. At high R_i values (in SUVs), it can be assigned to the motion of bound isolated monomers. At $R_i = 5$, this may be the motion of the small lipid-peptide particles evidenced by their low light scattering (see Fig. 2). The spread of correlation times to high values (not very different from infinite ones compared with fluorescence lifetimes) observed in the range of $R_i = 5$–40 may reflect the rotation of increasing-sized micelles or scattering bilayers (observed on Fig. 2) or the motion of bound self-associated peptides.

Tryptophan fluorescence quenching experiments

In an attempt to locate the tryptophanyl residues with respect to water and lipid microenvironments, quenching experiments with water- or lipid-soluble compounds were carried out with peptides in solution or bound to vesicles. Figure 8 depicts the quenching efficiency of Trp emission by Cs^+. Measurements were performed on δ-toxin ("hydrophilic" Trp15), peptides F and I ("hydrophobic" Trp16 and Trp5, respectively) in aqueous solution or bound to membranes at high lipid to peptide molar ratios ($R_i \approx 350$). Quenching of NATA in solution was used as a control; its Stern-Volmer plot (Fig. 8) is linear with a slope of 1.36 ± 0.03 M^{-1} and corresponds to a rate constant of quenching $k_Q = (4.6 \pm 0.1) \times 10^8$ M^{-1} s^{-1}, taking a lifetime $\tau_0 = 3$ ns for NATA in water without quencher (Ross et al. 1981).

Peptides in solution

The fluorescence of peptide I (Trp5) is much more quenched than that of δ-toxin (Trp15), peptide F (Trp16) or NATA. Stern-Volmer plots in the presence of peptides show curvatures and are analysed in terms of two parts of fluorescence, quenched and unquenched. As shown in Table 6, the Stern-Volmer constant for "hydrophobic" Trp5 and Trp16, which ought to be shielded in oligomers (according to their blue-shifted emission), are one order of magnitude greater than for the "hydrophilic" Trp15 of δ-toxin (tetrameric at this concentration, see Fig. 4) and NATA. As all lifetimes are smaller or similar to that of NATA, this indicates that Trp5 and Trp16 are over-quenched by Cs^+. This implies some affinity of Cs^+ for groups in the vicinity of these Trps. Asp4 might provide a site in peptide I and Asp18 for a residual non-helical fraction of peptide F (only 10% of its fluorescence is accessible). From Fig. 4, one can calculate the fraction f_i of the fluorescence intensity of δ-toxin (Trp15) related to each lifetime ($f_i = \alpha_i\tau_i / \Sigma\alpha_i\tau_i$).

Table 5 Variation of fluorescence anisotropy decay parameters of bound δ-toxin and analogue M as a function of the lipid to peptide molar ratio R_i. β_i and θ_i are the anisotropies and barycentres of the distribution profiles of rotational correlation times shown in Fig. 7

Peptide	Trp	R_i	β_1[a]	β_2	β_3	θ_2 (ns)	θ_3 (ns)	r_∞[c]
δ-Toxin	15	0	0.071	0.061	0.086	0.56	9.8	0
M[b]	16		0.089	0.033	0.053	0.94	8.4	0.043
δ-Toxin	15	5	0.115	0.072	0.031	3.2	27	0
M	16		0.096	0.046	0.076	1.6	27	0.022
δ-Toxin	15	20	0.110	0.065	0.043	3.4	32	0.006
M	16		0.095	0.035	0.088	1.7	34	0.029
δ-Toxin	15	40	0.092	0.070	0.056	2.3	13	0
M	16		0.081	0.039	0.098	1.3	24	0.027
δ-Toxin	15	120	0.042	0.132	0.044	2.7	16	€
M	16		0.053	0.069	0.096	1.5	21	0
δ-Toxin	15	150	0.036	0.158	0.024	3.0	39	0.005
M	16		0.045	0.074	0.099	1.3	19	0

[a] The actual initial anisotropy A_0 in 91% glycerol at –38 °C is 0.218 (Vincent et al. 1988). Total measured anisotropies are smaller than A_0. So, the fastest correlation time θ_1 (if unique) is not measured but its anisotropy is $\beta_1 = 0.218 - \sum_{i=2}^{n} \beta_i$

[b] Free peptide M at 5 μM shows an infinite anisotropy $r_\infty = 0.043$

[c] Infinite anisotropy or part of $\beta_3 \geq 50$ ns assumed similar to infinite anisotropy

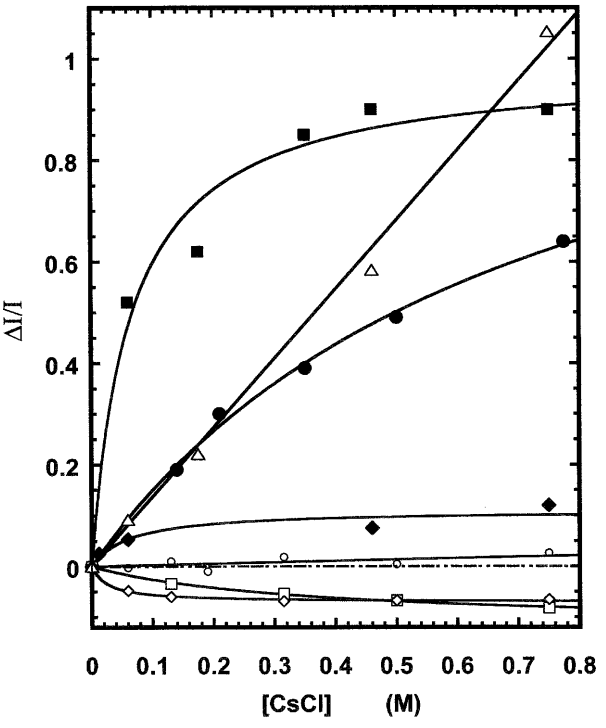

Fig. 8 Stern-Volmer plot of the quenching induced by CsCl on the Trp fluorescence of the different peptides. Curves are the best fit according to Eq. (8) (see Materials and methods). NATA (Δ), δ-toxin (●), peptide F (◆), peptide I (■) in solution at 2.6 ± 0.1 μM; (○) 2.6 μM δ-toxin + EPC vesicles, $R_i = 312$; (◇) 2.3 μM peptide F + EPC vesicles, $R_i = 355$; (□) 2.2 μM peptide I + EPC vesicles, $R_i = 370$. Fluorescence intensities were measured at the maximum of emission, $\lambda_{em} = 350$ nm for NATA, 340 nm for δ-toxin bound to lipids and 330 nm in all other cases. Excitation at 280 nm. Peptides were dissolved at least 6 h before the fluorescence measurements were performed, in 20 mM Tris-HCl buffer + 1 mM EDTA, pH = 7.5, at 25 °C

The fraction of Cs^+-sensitive fluorescence (0.55 ± 0.09) is close to the contribution (0.47) of τ_3 (4.5 ± 0.9 ns) to the emission. Then, assuming that the rotamer characterized by τ_3 is the quenchable species, a second-order collisional rate constant of $(6.9 \pm 2) \times 10^8$ M^{-1} s^{-1}, of the same order of magnitude as that found for NATA, is calculated (Ross et al. 1992). This is consistent with our scheme of oligomerization (Thiaudière et al. 1991) in which Trp15, on the hydrophilic side of the helix, should be partially exposed to the solvent (emission maximum at 340 nm) in the oligomeric state ($\theta = 6$ ns; see Fig. 5) present in our experimental conditions.

Peptides bound to lipid vesicles

A striking difference is observed since no Cs^+-quenching of the fluorescence of any of the peptides is obtainable. This indicates that all Trps are shielded from the aqueous solvent (Fig. 8). This is what was expected for Trp5 and Trp16 on the hydrophobic side of the helices, but it is also the case for Trp15 on the hydrophilic side. This implies that bound peptides are probably self-associated through their polar side and/or that Trp15 is sunk in the limit between the aliphatic chains of phospholipids and their polar head groups.

Since all Trps became inaccessible to water-soluble quencher, quenching by NO-labelled PC was assayed. One can therefore expect a severe quenching whose efficiency E, when plotted versus the lipid to inserted peptide ratio R_b', should be constant. This is not what is observed, as seen in Fig. 9A where, for NO-5PC, a drastic decrease of E is observed for all peptides, i.e. Trp5, Trp15 and Trp16. Then, according to the peptide concentration within the membrane, the relative positions of the Trps compared to NO-5 changed. This indicates a severe change in the orientation of peptides within the bilayer. At high peptide density ($R_b' \leq 40$), Trp5 is severely quenched by NO-5PC, while its fluorescence stays insensitive to NO-12PC. At low peptide density ($R_b' > 70$), it is quenched neither by NO-5PC nor by NO-12PC. It is therefore neither in contact with the hydrophobic core of the bilayer probed by doxyl-12 and doxyl-5 nor with the water-soluble Cs^+.

Table 6 Fluorescence quenching of δ-toxin and analogues F and I in aqueous solution in 20 mM Tris-HCl buffer (pH 7.5) + 1 mM EDTA. [Peptide] = 2.6 μM. NATA is measured for reference

Peptide	Trp	K (M^{-1})	f_a	f_3	τ_0 (ns)	k_Q (M^{-1} s^{-1})[a]
NATA	–	1.36 ± 0.03	1	–	3[b]	(4.6 ± 0.1) × 10^8
δ-Toxin	15	3.1 ± 0.3	0.55 ± 0.09	0.46[(c)]	4.5 ± 0.9[(c)]	(6.9 ± 2) × 10^8
F	16	18 ± 12	0.1 ± 0.13	–	–	–
I	5	30 ± 8	0.5 ± 0.25	–	–	–

[a] $k_Q = K/\tau_0$
[b] From Ross et al. (1981)
[c] Interpolated values from Fig. 4. The value τ_0 for δ-toxin in the absence of quencher is its longest lifetime τ_3. This choice has been made because of the similarity of f_a and f_3

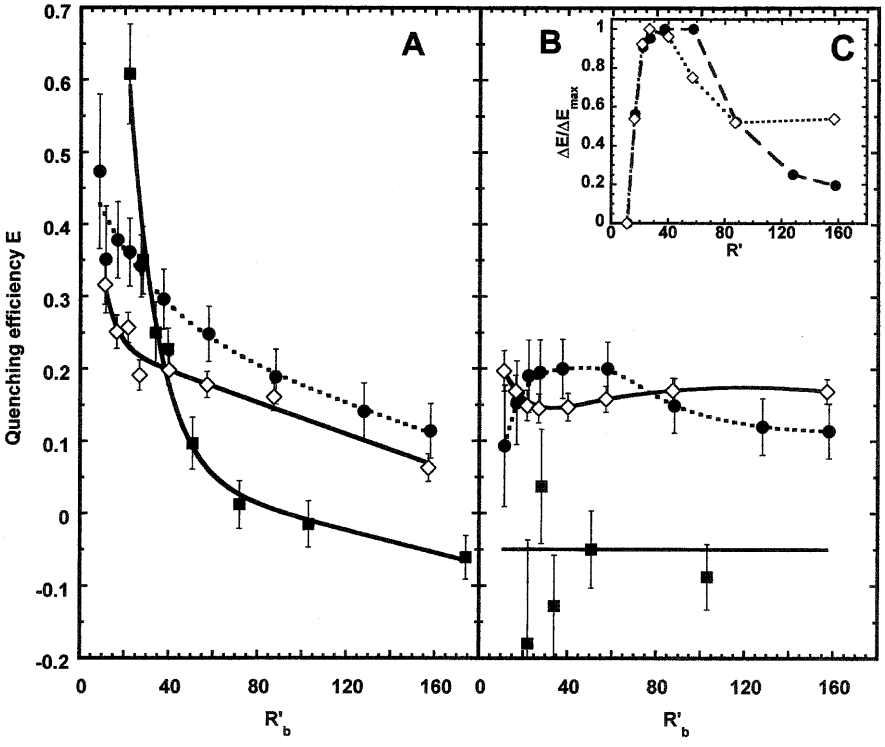

Fig. 9A–C Changes of the quenching efficiency E of δ-toxin and peptides F and I induced by doxyl groups at defined positions on phospholipid acyl chains: effects of these positions and of the surface density of inserted peptide. E is calculated according to Eq. (10) (see Materials and methods). **A** Effect of NO-5PC at 8.9 mol% in EPC vesicles; **B** effect of NO-12PC at 8.9 mol% in EPC vesicles. Insert **C**: normalized quenching efficiencies of δ-toxin and peptide F by NO-12PC. δ-Toxin (●), peptide F (◇), peptide I (■) at 2 μM. Other experimental conditions: see Fig. 8

A model can be proposed which is compatible with such experimental constraints, as shown in Fig. 10. Peptides of fraction α′ self-associated by the Trp5 domain could lie on the interface between the hydrophobic core and polar head groups of bilayers at low peptide density, and span the membrane and border its hydrophobic core on forming (1) pores in SUVs at moderate peptide density and (2) a ring around lipid discoid particles at high peptide density. If such a membrane-spanning complex is built, Trp16 would be located at a position intermediate between C5 and C12 of the phospholipid acyl chains, but closer to C5 in agreement with their respective efficiencies (Fig. 9A and B). This conclusion differs from the molecular modelling of a parallel helix bundle in a simplified lipid membrane model (Kerr et al. 1996), in which Trp15 and Trp16 are found confined just in the centre of the membrane. Our model can also explain the stronger quenching efficiency of Trp15 by NO-5PC than by NO-12PC. It is also in agreement with the higher sensitivity of Trp16 than Trp15 to the quenching by labelled lipids. Trp16, on the apolar side of the helix, should be in close contact with the acyl chains of the lipids, as opposed to Trp15 which is on the polar side. At low peptide density, Trp15 appears also to move off the C5 and C12 region while the distance C12-Trp16 becomes smaller than the distance C5-Trp16. This behaviour is still consistent with a change in peptide orientation from helices spanning the membrane to dimers (at least) of antiparallel helices lying flat on the bilayer in its fluid state, as proposed in Fig. 10. Such an antiparallel dimer should be strongly stabilized both by minimizing repulsive electrostatic interactions between the cluster of positive charges borne by the Lys of the C-terminal part and by favouring ion pairing between carboxylic and amino groups along the helices. Finally, the biphasic shape of the curves representing the quenching of Trp15 and Trp16 by NO-12PC (Fig. 9B), as well as the break in the negative slope of the

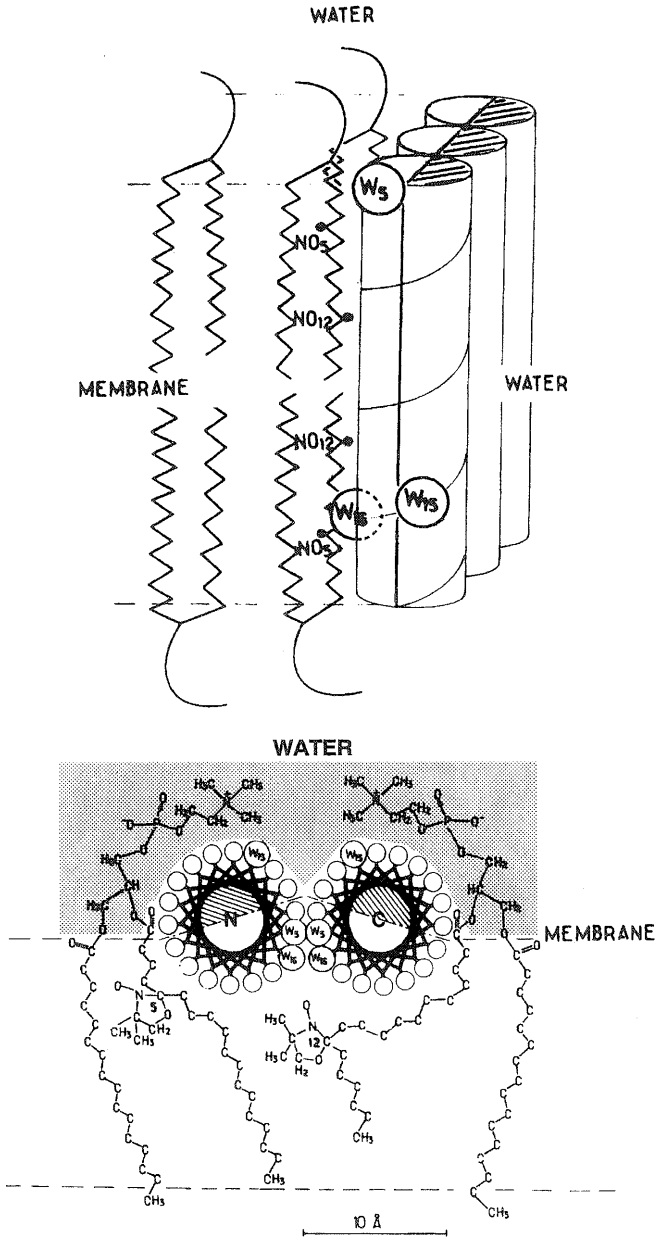

Fig. 10 Structural models compatible with the fluorescence data for peptides interacting with membranes. *Top*: at high peptide density in the bilayer ($R_b' \leq 40$), transmembrane peptides can border pores or fragments of membranes (Dufourcq et al. 1986) by protecting the acyl chains from the aqueous solvent. *Bottom*: at very low peptide density within the bilayer ($R_b' > 70$), peptides still self-associated lie flat at the interface between polar head groups (in grey) and the apolar core of the membrane. *Hatched areas* indicate the polar sides of helices. The positions of Trp residues are indicated

quenching curve of Trp16 by NO-5PC around $R_b' = 30$ (Fig. 9A), are indicative of an even more complex scheme of peptide rearrangements. At least a third intermediate location is necessary to account for these curves and may be the reason why the decreasing curves of Fig. 9A could not be fitted by a simple model with the spectroscopic characteristics of only the two orientational states described above, at high and low peptide density. The inserted Fig. 9C shows that, despite the low amplitudes of the changes in the quenching of Trp15 and Trp16 by NO-12PC compared with error bars, these changes, when normalized, are very similar at high peptide density up to $R_b' = 40$ and then diverge at lower densities. This indicates that Trp15 and Trp16 undergo anti-correlated displacements around C12 of the acyl chains up to $R_b' = 40$, followed by a swing to the laid flat interfacial location where Trp15, on the polar side of the helix, cannot yet come in contact with the acyl chains.

These different arrangements of δ-toxin and its analogues in lipids are sufficient to explain the complex changes observed in time-resolved fluorescence experiments in which most of the parameters show significant changes beyond $R_i = 40$ (or R_b' since there was no free peptide at these R_i in the presence of PS) or a transitory extremum between $R_i = 20$ and 40.

Conclusions

These experimental data provide some new insight into the aggregation processes of amphipathic α-helical δ-toxin and its analogues in solution, and into their mechanism of interaction with membranes.

In solution, the anisotropy decay data first confirm that these peptides self-aggregate in buffer solution as a function of their concentration, in agreement with other techniques (Kreger et al. 1971; Kantor et al. 1972; Fitton 1981; Thiaudière et al. 1991). Moreover, the new data obtained herein (emission maxima and lack of Cs^+-quenching) indicate directly that Trp5 and Trp16 on the apolar face of the helix lie on the interfaces between monomers in the oligomers.

However, the fact that Trp15, located on the hydrophilic side of the amphipathic helix, is only partly exposed to Cs^+ implies that a part of these hydrophilic sides contribute to the formation of the aggregates. This agrees with the decrease of the light scattering of peptide M induced by ionic strength and allows us to conclude that ion pairing has to be involved in this self-association mechanism. Such an association implies antiparallel α-helices allowing ionic interactions, probably between Asp4, 11 and 18 and Lys25 or 26, 22 and 14 respectively, as already postulated to explain the isodesmic linear aggregation of natural δ-toxin we previously observed (Thiaudière et al. 1991).

Finally, the position of the Trp in the sequence and the presence of Gly10 seem to be important features in the aggregation process. The anisotropy decay data indicate that peptide M exhibits large aggregates, characterized by an infinitely long rotational correlation time, whereas peptide I is present only as tetra- or pentamers at 2 μM (Table 4). Peptide M differs from peptide F by only a Gly10 → Leu substitution and an unformylated N-terminal Met. It is much more aggregated at low concentration and more α-helical. This agrees with the well-known conformational properties

of glycine residues (Creighton 1996). Thus, Gly10 could play a role in limiting the strong aggregation in solution which is correlated with the decreased haemolytic activity of peptide M observed by Alouf et al. (1989), despite this peptide generating channels in the black lipid membrane (BLM) similar to those of natural δ-toxin (Kerr et al. 1995).

For peptide organization in the bound state, the observations shown in this set of data lead to the conclusion that the interactions with the phospholipidic membrane strongly disturb both the hydrophilic and the hydrophobic surfaces of the water-soluble aggregates. This must be achieved by a process of dissociation of aggregates following the primary interaction at the membrane surface. As a function of the lipid to inserted peptide ratio R_b', different self-associated forms occur, in agreement with predictions from energy calculations (Raghunathan et al. 1990).

At low peptide concentration in the bilayer ($R_b' > 70$), at least dimers with antiparallel α-helices are likely to occur according to the quenching data; they lie flat at the interface between acyl chains and polar heads as proposed in Fig. 10 (bottom). All the Trp positions are shielded from water and stay far from C5 of the acyl chains, because they are in the vicinity or directly (Trp5) involved in the self-association domains. The most hydrophobic position, Trp16, may be closer to C12 than to C5 because neighbouring lipids should adopt very disordered conformations of their aliphatic chains in order to fill the free space left under the helices. This agrees with the very significant disordering of acyl chains induced by natural δ-toxin and detected by NMR (Dufourc et al. 1990).

High peptide concentration in lipids ($R_b' \leq 20$) favours higher degrees of self-association, as shown by quasi-infinite correlation times. It induces also the disruption of SUVs into small, weakly scattering particles. According to quenching experiments, Trp5 and Trp16 come in close contact with C5 of the acyl chains while Trp16 is further from C12 and Trp5 is quite beyond it. Trp15 is always further from C12 and C5 than is Trp16. This implies that the amphipathic helices must span the membrane, with their hydrophobic sectors facing the aliphatic chains of phospholipids and their polar sides being in a more polar environment (Fig. 10, top). Keeping in mind that polar media are quenching media, which thus shortens lifetimes, this is particularly obvious for peptides at 5 μM for which the shortest lifetime of the "hydrophobic" Trp16 disappears to the benefit of the longest one, whilst the weights of the different lifetimes of the "hydrophilic" Trp15 change weakly. This is also confirmed at 20 μM, where these changes are all the greater as the Trp is more "hydrophobic", i.e. Trp15 ("hydrophilic" side of the helix), Trp5 (near the end of the hydrophobic side of the helix) and Trp16 (in its middle). Such a structural model presents two different aspects: either peptide bundles with a hydrophilic core which allows pore formation in scattering vesicles (between $R_i = 20$ and 40) as already proposed from BLM experiments (Kerr et al. 1995), or, with opposite curvature, a belt of amphipathic peptides covering the aliphatic section of membrane fragments. This last description fits with the decrease in the light scattering observed herein at $R_i \leq 7$ and it is coherent with the very recent X-ray and NMR data from Lohner et al. (1999) at $R_i = 15$ with DMPC and with what was observed by NMR of lipids with δ-toxin around $R_i = 5$ by Dufourc et al. (1990) and Rydall and Macdonald (1992).

The change in orientation of the axes of α-helical peptides (from parallel to perpendicular with respect to the bilayer surface) on decreasing the lipid to peptide molar ratio has been already characterized on hydrated oriented bilayers in a fluid phase in the case of alamethicin-diphytanoyl-PC at $R_i = 120$ (but not with dioleoyl-PC) (Huang and Wu 1991), and magainin-dimyristoyl-(PC-PG) at $R_i = 30$ (Ludtke et al. 1994). At small R_i values (10–15), melittin has also been shown to span oriented bilayers (Smith et al. 1994), while δ-toxin seems to have no preferred orientation in the gel phase (Brauner et al. 1987). Such a change in orientation we observe here with fluid SUVs should be a general feature in the function of cytotoxic amphipathic peptides (Bechinger 1999). Such membrane structural changes imply the leakage or lysis of SUVs, already documented by Morgan et al. (1986) and Freer et al. (1984), and bacteria in the case of magainin (Ludtke et al. 1994). This also occurs under conditions, peptide concentrations and R_i values, similar to those required for haemolysis by natural δ-toxin (Alouf et al. 1989).

Acknowledgements The technical staff of LURE are acknowledged for running the synchrotron machine during the beam sessions. We are indebted to Dr. A. Zackowski (Institut de Biologie Physico-Chimique, Paris) for providing us with the 5-doxyl derivative of phosphatidylcholine.

References

Alouf JE, Dufourcq J, Siffert O, Thiaudière E, Geoffroy C (1989) Interaction of staphylococcal δ-toxin and synthetic analogues with erythrocytes and phospholipid vesicles. Biological and physical properties of the amphipathic peptides. Eur J Biochem 183: 381–390

Bechinger B (1999) The structure, dynamics and orientation of antimicrobial peptides in membranes by mutidimensional solid-state NMR spectroscopy. Biochim Biophys Acta 1462: 157–183

Brauner JW, Mendelsohn R, Prendergast FG (1987) Attenuated total reflectance Fourier transform infrared studies of the interaction of melittin, two fragments of melittin, and δ-hemolysin with phosphatidylcholines. Biochemistry 26: 8151–8158

Chen Y, Barkley MD (1998) Toward understanding tryptophan fluorescence in proteins. Biochemistry 37: 9976–9982

Creighton TE (1996) Proteins: structure and molecular properties. Freeman, New York

Dawson CR, Drake AF, Helliwell J, Hider RC (1978) The interaction of bee melittin with lipid bilayer membranes. Biochim Biophys Acta 510: 75–86

DeGrado WF, Kézdy FJ, Kaiser ET (1981) Design, synthesis and characterization of a cytotoxic peptide with melittin-like activity. J Am Chem Soc 103: 679–681

Dufourc EJ, Dufourcq J, Birkbeck TH, Freer JH (1990) δ-Haemolysin from *Staphylococcus aureus* and model

membranes. A solid state ^{2}H-NMR and ^{31}P-NMR study. Eur J Biochem 187: 581–587

Dufourcq J, Faucon JF, Fourche G, Dasseux JL, Le Maire M, Gulik-Krzywicki T (1986) Morphological changes of phosphatidylcholine bilayers induced by melittin: vesicularization, fusion, discoidal particles. Biochim Biophys Acta 859: 33–48

Dufourcq J, Castano S, Talbot JC (1999) δ-Toxin, related haemolytic toxins and peptide analogues. In: Alouf JE, Freer JH (eds) The comprehensive sourcebook of bacterial protein toxins. Academic Press, London, pp 386–401

Eisenberg D, Weiss RM, Terwilliger TC, Wilcox W (1982) Hydrophobic moments and protein structure. Faraday Symp Chem Soc 17: 109–120

Fitton JE (1981) Physicochemical studies on δ-haemolysin, a staphylococcal cytolytic polypeptide. FEBS Lett 130: 257–260

Freer JH, Birkbeck TH (1982) Possible conformation of δ-lysin, a membrane damaging peptide of *Staphylococcus aureus*. J Theor Biol 94: 535–540

Freer JH, Birkbeck TH, Bhakoo M (1984) Interaction of staphylococcal δ-lysin with phospholipid monolayers and bilayers. In: Alouf JE (ed) Bacterial protein toxin. Academic Press, London, pp 181–189

Gallay J, Vincent M, Nicot C, Waks M (1987) Conformational aspects and rotational dynamics of synthetic adrenocorticotropin-(l–24) and glucagon in reverse micelles. Biochemistry 26: 5738–5747

Garone L, Fitton JE, Steiner RF (1988) The interaction of δ-haemolysin with calmodulin. Biophys Chem 31: 231–245

Gentin M, Vincent M, Brochon JC, Livesey AK, Cittanova N, Gallay J (1990) Time-resolved fluorescence of the single tryptophan residue in rat α-fetoprotein and rat serum albumin: analysis by the maximum entropy method. Biochemistry 29: 10405–10412

Huang HW, Wu Y (1991) Lipid-alamethicin interactions influence alamethicin orientation. Biophys J 60: 1079–1087

Ichiye T, Karplus M (1983) Fluorescence depolarization of tryptophan residues in proteins: a molecular dynamics study. Biochemistry 22: 2884–2893

John E, Jähnig F (1988) Dynamics of melittin in water and membrane as determined by fluorescence anisotropy decay. Biophys J 54: 817–827

Kantor HS, Temples B, Shaw WV (1972) Staphylococcal δ-hemolysin: purification and characterisation. Arch Biochem Biophys 151: 142–156

Katsu T, Ninomya C, Kuroko M, Kobayashi M, Hirota T, Fujita Y (1988) Action mechanism of amphipathic peptides gramicidin S and melittin on erythrocyte membrane. Biochim Biophys Acta 939: 57–63

Katsu T, Kuroko M, Morikawa T, Sanchika K, Fujita Y, Yamamura H, Uda M (1989) Mechanism of membrane damage induced by the amphipathic peptides gramicidin S and melittin. Biochim Biophys Acta 983: 135–141

Kawato S, Kinosita K Jr, Ikegami A (1977) Dynamic structure of lipid bilayers studied by nanosecond fluorescence techniques. Biochemistry 16: 2319–2324

Kerr ID, Dufourcq J, Rice JA, Fredkin DR, Sansom MSP (1995) Ion channel formation by synthetic analogues of staphylococcal δ-toxin. Biochim Biophys Acta 1236: 219–227

Kerr ID, Doak DG, Sankararamakrishnan R, Breed J, Sansom MSP (1996) Molecular modelling of staphylococcal δ-toxin ion channels by restrained molecular dynamics. Protein Eng 9: 161–171

Kinosita K Jr, Kawato S, Ikegami A (1977) A theory of fluorescence polarisation decay in membranes. Biophys J 20: 289–305

Kreger AS, Kim S, Zaboretzky F, Bernheimer AV (1971) Purification and properties of staphylococcal δ-hemolysin. Infect Immun 3: 449–465

Kuipers OP, Vincent M, Brochon JC, Verheij HM, de Haas GH, Gallay J (1991) Insight into the conformational dynamics of specific regions of porcine pancreatic phospholipase A_2 from a time-resolved study of a genetically inserted single tryptophan residue. Biochemistry 30: 8771–8785

Lee KE, Fitton JE, Wüthrich K (1987) NMR investigation of the conformation of δ-haemolysin bound to dodecylphosphocholine micelles. Biochim Biophys Acta 911: 144–153

Li De la Sierra IM, Vincent M, Padron G, Gallay J (1992) Interaction of recombinant human epidermal growth factor with phospholipid vesicles. A steady-state and time-resolved fluorescence study of the bis-tryptophan sequence (Trp49-Trp50). Eur Biophys J 21: 337–344

Lipari G, Szabo A (1982) Model-free approach to the interpretation of nuclear magnetic resonance relaxation in macromolecules. I. Theory and range of validity. J Am Chem Soc 104: 4546–4559

Livesey AK, Brochon JC (1987) Analysing the distribution of decay constants in pulse-fluorimetry using the maximum entropy method. Biophys J 52: 693–706

Livesey AK, Delaye M, Licinio P, Brochon JC (1987) Maximum entropy analysis of dynamic parameters via the Laplace transform. Faraday Discuss Chem Soc 83: 1–12

Lohner K, Staudegger E, Prenner EJ, Lewis RNAH, Kriechbaum M, Degovics G, McElhaney RN (1999) Effect of staphylococcal δ-lysin on the thermotropic phase behavior and vesicle morphology of dimyristoylphophatidylcholine lipid bilayer model membranes. Differential scanning calorimetric, ^{31}P nuclear magnetic resonance and Fourier transform infrared spectroscopic, and X-ray diffraction studies. Biochemistry 38: 16514–16528

Ludtke SJ, He K, Wu Y, Huang HW (1994) Cooperative membrane insertion of magainin correlated with its cytolytic activity. Biochim Biophys Acta 1190: 181–184

Mellor IR, Thomas DH, Sansom MSP (1988) Properties of ion channels formed by *Staphylococcus aureus* δ-toxin. Biochim Biophys Acta 942: 280–294

Merola F, Rigler R, Holmgren A, Brochon JC (1989) Picosecond tryptophan fluorescence of thioredoxin: evidence for discrete species in slow exchange. Biochemistry 28: 3383–3398

Morgan CG, Fitton JE, Yianni YP (1986) Fusogenic activity of δ-haemolysin from *Staphylococcus aureus* in phospholipid vesicles in the liquid-crystalline phase. Biochim Biophys Acta 863: 129–138

O'Neil KT, Wolfe HR Jr, Erickson-Vitanen S, de Grado WF (1987) Fluorescence properties of calmodulin binding peptides reflect α-helical periodicity. Science 236: 1454–1456

Raghunathan G, Seetharamulu P, Brooks BR, Guy HR (1990) Models of δ-hemolysin membrane channels and crystal structures. Proteins 8: 213–225

Ross JBA, Rousslang KW, Brand L (1981) Time-resolved fluorescence and anisotropy decay of the tryptophan in adrenocorticotropin-[1–24]. Biochemistry 20: 4361–4369

Ross JBA, Wyssbrod HR, Porter RA, Schwartz GP, Michaels CA, Law WR (1992) Correlation of tryptophan fluorescence intensity decay parameters with ^{1}H NMR-determined rotamer conformations: [Tryptophan^{2}]oxytocin. Biochemistry 31: 1585–1594

Rydall JR, Macdonald PM (1992) Influence of staphylococcal δ-toxin on the phosphatidylcholine head group as observed using ^{2}H-NMR. Biochim Biophys Acta 1111: 211–220

Singleton WS, Gray MS, Brown ML, White JL (1965) Chromatographically homogeneous lecithin from egg phospholipids. J Am Oil Chem Soc 42: 53–56

Smith R, Separovic F, Milne TJ, Whittaker A, Bennett FM, Cornell BA, Makriyannis A (1994) Structure and orientation of the pore forming peptide, melittin, in lipid bilayers. J Mol Biol 241: 456–466

Thiaudière E (1990) Relation structure-activité de peptides amphiphiles cytolytiques. Etude de la toxine-δ de *Staphylococcus aureus* et d'analogues synthétiques, en solution aqueuse et à l'état lié aux lipides. Thèse de Doctorat, Université de Bordeaux l, France

Thiaudière E, Siffert O, Talbot JC, Bolard J, Alouf JE, Dufourcq J (1991) The amphiphilic α-helix concept. Consequences on the structure of staphylococcal δ-toxin in solution and bound to lipids. Eur J Biochem 195: 203–213

Vincent M, Gallay J (1991) The interaction of horse heart apocytochome *c* with phospholipid vesicles and surfactant micelles: time-resolved fluorescence study of the single tryptophan residue (Trp-59). Eur Biophys J 20: 183–191

Vincent M, Brochon JC, Merola F, Jordi W, Gallay J (1988) Nanosecond dynamics of horse heart apocytochome *c* in aqueous solution as studied by time-resolved fluorescence of the single tryptophan residue (Trp-59). Biochemistry 27: 8752–8761

Vogel H, Nilsson L, Rigler R, Voges KP, Jung G (1988) Structural fluctuations of helical polypeptide traversing a lipid bilayer. Proc Natl Acad Sci USA 85: 5067–5071

Wahl P (1975) Nanosecond pulse fluorimetry. In: Pain M, Smith B (eds) New techniques in biophysics and cell biology, vol 2. Wiley, Chichester, pp 233–285

Weaver AJ, Kemple MD, Brauner JW, Mendelsohn R, Prendergast FG (1992) Fluorescence, CD, attenuated total reflectance (ATR) FTIR, and ^{13}C NMR characterization of the structure and dynamics of synthetic melittin and melittin analogues in lipid environments. Biochemistry 31: 1301–1313

Yguerabide J (1972) Nanosecond fluorescence spectroscopy of macromolecules. Methods Enzymol 26: 498–578